First publ. in: Journal of Molecular Medicine 3 (1997), 11, pp. 750-764

Caspase-Mediated Apoptosis in Neuronal Excitotoxicity Triggered by Nitric Oxide

Marcel Leist, Christiane Volbracht, Simone Kühnle, Eugenio Fava, Elisa Ferrando-May, and Pierluigi Nicotera
Department of Molecular Toxicology, Faculty of Biology, University of Konstanz, Konstanz, Germany

ABSTRACT

Background: Excitotoxicity and excess generation of nitric oxide (NO) are believed to be fundamental mechanisms in many acute and chronic neurodegenerative disorders. Disturbance of Ca^{2+} homeostasis and protein nitration/nitrosylation are key features in such conditions. Recently, a family of proteases collectively known as caspases has been implicated as common executor of a variety of death signals. In addition, overactivation of poly-(ADP-ribose) polymerase (PARP) has been observed in neuronal excitotoxicity. We therefore designed this study to investigate whether triggering of caspase activity and/or activation of PARP played a role in cerebellar granule cell (CGC) apoptosis elicited by peroxynitrite ($ONOO^-$) or NO donors.
Materials and Methods: CGC from wild-type or PARP −/− mice were exposed to various nitric oxide donors. Caspase activation and its implications for membrane alterations, Ca^{2+} homeostasis, intracellular proteolysis, chromatin degradation, and cell death were investigated.
Results: CGC exposed to NO donors undergo apoptosis, which is mediated by excess synaptic release of excitotoxic mediators. This excitotoxic mechanism differs from direct NO toxicity in some other neuronal populations and does not involve PARP activation. Inhibition of caspases with different peptide substrates prevented cell death and the related features, including intracellular proteolysis, chromatin breakdown, and translocation of phosphatidylserine to the outer surface of the cell membrane. Increased Ca^{2+} influx following N-methyl-D-aspartate (NMDA) receptor (NMDA-R) activation was not inhibited by caspase inhibitors.
Conclusions: In CGC, NO donors elicit apoptosis by a mechanism involving excitotoxic mediators, Ca^{2+} overload, and subsequent activation of caspases.

INTRODUCTION

In the central nervous system, nitric oxide (NO) is a pleiotropic messenger molecule involved in the regulation of blood flow and cellular signalling (1–3). However, experiments using inhibitors of nitric oxide synthase (NOS) and studies performed in gene-targeted mice, which lack different isoforms of NOS, suggest that NO production is also involved in various neuropathological processes (4–9).

To explain the apparent dichotomy between physiological and pathological effects of NO, it has been proposed that its reaction products may have contrasting effects (1,5,10,11). For example, formation of peroxynitrite ($ONOO^-$) from $NO^\cdot$ and $O_2^{-\cdot}$ would in most cases be detrimental, whereas S-nitrosylation of proteins by $NO^\cdot$ or other NO-related species would regulate physiological functions. Thus, hemoglobin nitrosylation has a role in the fine-tuning of cerebral oxygen supply (12), and nitric oxide may trigger Ca^{2+}-independent neurotransmitter release by S-nitrosylation of synaptic proteins (13,14).

Many toxic effects of NO or its reaction products have been attributed to processes not encountered under physiologic conditions, i.e., inactivation or inhibition of proteins (3,15) and DNA damage (16). However, it is becoming clear that inadequate or excessive stimulation of NO's normal regulatory functions can also elicit cytotoxicity. One example is the NO-induced apopto-

Address correspondence and reprint requests to: Prof. P. Nicotera, Chair of Molecular Toxicology, Faculty of Biology, University of Konstanz, Box X911, D-78457 Konstanz, Germany. Phone: +49-7531-884035; Fax: +49-7531-884033; E-mail: pierluigi.nicotera@uni-konstanz.de

sis of cerebellar granule cells (CGC). Here, cytotoxicity seems to result from excessive stimulation of neurotransmitter release (17), which may be caused by S-nitrosylation of synaptic proteins involved in the regulation of exocytosis (13,14). Consequently, CGC apoptosis elicited by $NO/ONOO^-$ requires the activation of the *N*-methyl-D-aspartate receptor (NMDA-R) and a receptor-dependent increase of the intracellular free calcium concentration ($[Ca^{2+}]_i$) (17,18). Therefore, this model allows the study of excitotoxicity based on the release of endogenous glutamate-receptor agonists from presynaptic sites.

Excitotoxicity and the resulting imbalance of neuronal Ca^{2+} homeostasis have been extensively studied (19–21). Nevertheless, the downstream mechanisms coupling increased $[Ca^{2+}]_i$ to cell death are still poorly understood. Potential targets of Ca^{2+} include kinases, phosphatases, proteases, phospholipases, nitric oxide synthase, and mitochondria (19–22). It has often been assumed that a generalized, nonspecific breakdown of cellular homeostatic mechanisms would lead to necrotic/lytic cell death (23). More recent evidence has shown that an ordered sequence of events leading to apoptosis is induced by low concentrations of excitotoxins, whereas high concentrations elicit necrosis (24). It seems that excitotoxin-challenged cells, which are able to maintain for some time mitochondrial function and ATP production, die by apoptosis, whereas neurons that do not maintain sufficient energy production for the completion of the apoptotic program lyse necrotically (25,26). These findings are corroborated by in vivo observations in stroke models, in which apoptosis is observed in the border regions and necrosis dominates in the more severely stressed cells of the ischemic core (27–30).

In most cases of apoptotic cell death, activation of proteases of the caspase family seems to play a central role (31,32). In CGC, inactive caspase precursors are constitutively expressed and their activation has been demonstrated during apoptosis induced by K^+ withdrawal (33–35). Caspase inhibitors have also been shown in vivo to reduce ischemic, traumatic, and excitotoxic damage (36–38), but because of the complexity of the in vivo models, it has remained unclear whether inhibition of caspases protects neurons from the toxic consequences of disturbed $[Ca^{2+}]_i$ homeostasis or from a putative induction of interleukin-1-beta (IL-1β) formation (39) or other mediators.

This question was addressed in the present study using a model system of NO-induced autocrine excitotoxicity in CGC. We studied whether $[Ca^{2+}]_i$ overload following NO-dependent glutamate receptor stimulation would cause neuronal apoptosis by a mechanism involving activation of poly-(ADP-ribose)-polymerase (PARP) (16) and/or caspases.

MATERIALS AND METHODS

Materials

Cell culture dishes were purchased from Greiner (Frickenhausen, Germany) and cell culture media from Life Technologies (Eggenstein, Germany) or Biochrome (Berlin, Germany). Acetoxymethyl esters of fluo-3 (fluo-3-AM), fura-2-AM, calcein-AM, SYTOX, ethidium homodimer-1 (EH-1), and H-33342 were obtained from Molecular Probes (Eugene, OR). Peroxynitrite, S-nitrosoglutathione (GSNO), *S*-nitroso-*N*-acetyl-penicillamine (SNAP) and *S*-nitrosocysteine (SNOC) were synthesized and quantitated as described previously (40–43). DEA NONOate and spermine NONOate were from Alexis Corporation. The caspase substrate DEVD-aminotrifluoromethylcoumarine (–afc) and 6,7-dichloroquinoxaline-2,3-dione (DCQX) were obtained from Biomol (Hamburg, Germany). (+)-5-methyl-10,11-dihydro-5H-dibenzo[a,d]cyclo-hepten-5,10-imine (MK801) came from RBI (Biotrend Chemikalien GmbH, Köln, Germany). Succinyl-Leu-Leu-Val-Tyr-aminomethylcoumarine (succ-LLVY-amc), calpain inhibitors I, II, and III (Ac-Leu-Leu-L-norleucinal, Ac-Leu-Leu-L-methional, z-Val-L-phenylalaninal), z-Phe-chloromethylketone (cmk), and the caspase inhibitors DEVD-CHO, z-VAD-fluoromethylketone (fmk), Ac-YVAD-cmk or Ac-YVAD-2,6-dimethylbenzoyloxymethylketone (ICE II), and z-D-2,6-dichlorobenzoyloxymethylketone (cbk) (ICE III) were obtained from Bachem Biochemica GmbH (Heidelberg, Germany). DEVD-fmk was from Enzyme Systems (Dublin, CA). Solvents and inorganic salts were from Merck (Darmstadt, Germany) or Riedel-de Haen (Seelze, Germany). All other reagents not further specified were from Sigma (Deisenhofen, Germany).

Animals

PARP (–/–) mice (C57B1/6 × 129/Sv background) or corresponding wild-type animals

were generously provided by Dr. Zhao-Qi Wang (IARC, Lyon, France) (44). All animals used for cell preparations were typed by Southern blot (44) to verify the genotype. For other experiments, 8-day-old specific, pathogen-free BALB/c mice were obtained from the Animal Unit of the University of Konstanz. All experiments were performed in accordance with international guidelines to minimize pain and discomfort (NIH guidelines and European Community Council Directive 86/609/EEC).

Cell Culture

CGC were prepared as described (45). Neurons were plated on 50 μg/ml (250 μg/ml for glass surfaces) poly-L-lysine (MW >300 kDa) coated dishes at a density of about 0.25×10^6 cells/cm^2 [800,000 cells/ml; 500 μl/well (24-well plate)] and cultured in Eagle's basal medium (BME, Gibco) supplemented with 10% heat-inactivated fetal calf serum, 20 mM KCl, 2 mM L-glutamine, and penicillin-streptomycin. Forty-eight hours after plating, cytosine arabinoside (10 μM) was added to the cultures. Neurons were routinely used at 8–10 days in vitro (DIV) unless otherwise indicated. Glial fibrillary acid protein-positive cells were less than 5%. Cultures were exposed to NO donors in their own medium. Usually culture medium was exchanged for a controlled salt solution (CSS) [120 mM NaCl, 25 mM hydroxyethyl-piperazylsulfonic acid (HEPES); 15 mM glucose; 25 mM KCl; 1.8 mM $CaCl_2$; 2 mM $MgCl_2$] 4 hr after the start of the incubation and the cells were left in this medium without re-addition of any inhibitors. Solvents alone (up to 0.4% DMSO were added to cultures) did not affect neuronal survival in either way. Inhibitors were added routinely 30 min before exposure to NO donors.

Cytotoxicity Assays

To assess plasma membrane integrity and nuclear morphological changes, CGC were loaded with 0.5 μM calcein-AM for 5 min (cells with intact membranes displayed green fluorescence) in the presence of 1 μM ethidium homodimer-1 (EH-1) (cells with broken membranes exhibit nuclear red fluorescence) and 500 ng/ml of the bisbenzimide dye H-33342 (cell permeant, blue-fluorescent). Alternatively, apoptosis and secondary lysis were quantitated by double-staining neuronal cultures with 1 μg/ml H-33342 and 0.5 μM SYTOX (non-cell permeant, green-fluorescent). Apoptotic cells were characterized by condensed, highly fluorescent nuclei. Each data point corresponds to 200 to 600 cells that were scored. In addition, the percentage of viable cells was quantitated by their 3-(4,5-dimethylthiazole-2-yl)-2,5-diphenyltetrasodium bromide (MTT)-reducing capacity after incubation with 0.5 mg/ml MTT for 60 min (46).

Ca^{2+} Measurements

The free intracellular Ca^{2+} concentration ($[Ca^{2+}]_i$) was measured by imaging individual neurons loaded with fluorescent Ca^{2+} indicators. To routinely study changes of $[Ca^{2+}]_i$, CGC were loaded in their original medium with 1 μM fluo-3-AM for 10 min at 37°C (17). The medium was then exchanged for CSS, in which CGC were incubated for 5 min to allow complete de-esterification of fluo-3. The medium was exchanged again for the original neuron-conditioned, complete BME medium supplemented with 20 mM HEPES (GSNO as stimulus) or for CSS (without Mg^{2+}) (50 μM glutamate or 200 μM NMDA as stimulus) or for CSS *plus* 2 μM MK801 (200 μM kainate as stimulus). CGC were allowed to equilibrate at room temperature for 10 min before the exposure. Images were collected using the 488-nm excitation and 520-nm emission wavelengths and a Leica DM-IRB microscope equipped with a 40× lens. Data from 10–20 neurons were recorded at 3- to 10-sec intervals either with a Leica TCS 4D confocal system, or with a Dage-72 (Dage-MTI, Michigan City, IN) CCD camera [756 (H) × 581 (V) pixels] coupled to a videoscope GEN-III image intensifier. Videomicroscopy data were analyzed using software from Imaging Corporation (St. Catherines, Ontario, Canada). Relative mean fluorescence levels from defined areas corresponding to the position of neuronal cell bodies were recorded over 20 min and further processed using Excel 5.0 (Microsoft, Seattle, WA). The mean fluorescence level of each marked cell was arbitrarily set to 1 at the beginning of each experiment. Absolute $[Ca^{2+}]_i$ was measured by videoimaging after loading with 2.5 μM fura-2-AM (Molecular Probes, Eugene, OR) as described earlier (47). A Leica DM-IRB microscope equipped with a computer-controlled filter wheel (Sutter, Novato, CA) and quartz optics was used for imaging (λ_{ex-1} = 340 nm, λ_{ex-2} = 380 nm, λ_{em} = 505 nm). $[Ca^{2+}]_i$ was determined by in situ calibration using the equation $[Ca^{2+}]_i = K_d \times (R - R_{min})/(R_{max} - R) \times S_{f2}/S_{b2}$, with $K_{d(25°C)}$ = 264

nM (48). To determine R_{min} cells were washed twice with calibration buffer [120 mM NaCl, 25 mM HEPES, 15 mM glucose, 25 mM KCl, 2 mM $MgCl_2$, 2 mM ethylene glycol-bis (β-aminoethyl ether) N,N,N',N'-tetraacetic acid (EGTA)] and equilibrated for 20 min in calibration buffer supplemented with 5 μM ionomycin. Ca^{2+} (5 mM) and ionomycin (10 μM) were added to saturate fura-2 with Ca^{2+} and calculate R_{max}. Autofluorescence was measured after addition of 5 mM $MnCl_2$.

Electrophoretic Assays

Fodrin proteolysis was analyzed by immunoblot (49). CGC cultures were lysed in RIPA buffer (150 mM NaCl, 50 mM Tris, 1% NP-40, 0.25% sodium deoxycholate, 1 mM EGTA) supplemented with protease inhibitors [1 mM phenylmethylsulfonyl fluoride (PMSF), 1 mM benzamidine, 1 mM iodoacetate, 1 mM iodoacetamide, 40 μM leupeptin, 10 μg/ml antipain, 5 μg/ml pepstatin]. Before lysis, cultures were stained with 0.5 μM SYTOX to control the percentage of cells with intact membranes, which was over 95% for all samples analyzed. Protein was determined using the bicinchonic acid method (Bio-Rad, München, Germany) and 5 μg protein/lane was loaded on 8% polyacrylamide gels. Proteins were separated under reducing conditions at 60 mA and then blotted on a nitrocellulose membrane (Amersham-Buchler, Braunschweig, Germany) in a Bio-Rad semidry blotter at 2.6 mA/cm^2 for 50 min using a Towbin buffer system. Blots were blocked for 1 hr and then incubated with anti-fodrin monoclonal antibody (clone #1622, 1:1000) from Chemicon (Temecula, CA) diluted in TNT (150 mM NaCl, 50 mM Tris, pH 8.0, 0.05% Tween 20) for 1 hr at room temperature. Specifically stained bands were detected by chemiluminescence (Amersham) using a peroxidase-coupled secondary antibody.

Field inversion gel electrophoresis (FIGE) was performed as described previously (18,25). About 1.5×10^6 cells (corresponding to 1 well of a 12-well plate) were embedded into 40-μl agarose blocks. Lambda-DNA concatemers ($n \times 50$ kbp) were used as molecular weight markers.

Enzymatic Assays

Caspase activity (DEVD-afc cleavage) was assayed as described before (50,51) with the following modifications: CGC were pelleted in phosphate buffered saline (PBS), supplemented with 5 mM EDTA, 1 μg/ml leupeptin, 1 μg/ml pepstatin, 1 μg/ml aprotinin, 1 mM PEFA block. They were lysed in 25 mM HEPES, 5 mM $MgCl_2$, 1 mM EGTA, 0.5% Triton X-100, 1 μg/ml leupeptin, 1 μg/ml pepstatin, 1 μg/ml aprotinin, and 1 mM PEFA block, pH 7.5. The fluorimetric assay was performed in microtiter plates with a substrate concentration of 40 μM and a total protein amount of 5 μg. Cleavage was followed in reaction buffer (50 mM HEPES, 10 mM DTT, 1% sucrose, 0.1% CHAPS) over a period of 30 min at 37°C with λ_{ex} = 390 nm and λ_{em} = 505 nm and the activity was calibrated with afc-standard solutions. One unit was defined as formation of 1 pmol AFC/min. Control experiments were also performed, in which DTT was removed from the reaction buffer to avoid false negative results due to possible reduction of nitrosylated thiols.

Calpain activity was determined by a kinetic fluorimetric assay using 100 μM suc-LLVY-amc as calpain substrate. Briefly, purified rabbit skeletal muscle calpain (0.75 U/ml final concentration) was dissolved in assay buffer [50 mM Tris, 8 mM dithiothreitol (DTT), and various inhibitors to be tested]. The reaction was started by the addition of 2 mM $CaCl_2$ (final concentration) *plus* the fluorogenic substrate. Linear fluorescent increases were monitored at λ_{ex} = 380 nm and λ_{em} = 442 nm for 30 min. When DEVD-afc was used as alternative substrate, no activity was measured.

Microscopy

Cells stained with different fluorescent probes were imaged on Leica DM-IRB microscopes equipped with a video camera or connected to a TCS-4D UV/VIS confocal scanning system (Leica AG, Benzheim and Leica Lasertechnik, Heidelberg, Germany). Staining of cells with fluorescein-conjugated annexin V was performed as initially described (52) with the following modifications: CGC were grown on glass-bottomed culture dishes and incubated with GSNO and various inhibitors. After the incubation, 0.5 μg/ml H-33342 was added to the cultures to later visualize chromatin structure. After 10 min incubation at 37°C, CGC were washed for 10 sec with binding buffer (10 mM HEPES, 140 mM NaCl, 2.5 mM $CaCl_2$, 10 mM $MgCl_2$) and subsequently incubated for 2 min in the dark with annexin V solution (Boehringer-Mannheim, Mannheim, Germany) diluted 1:70 in binding buffer. Following a new wash with binding buffer, stained cultures were immersed in bind-

ing buffer supplemented with 0.25 μM ethidium homodimer-1 and visualized by 3-channel (blue: chromatin-structure, green: annexin-binding, red: membrane-integrity) confocal microscopy using a 63 × /NA1.32 UV-corrected lens. Alternatively, cultures were fixed after the annexin staining step with 3.7% formaldehyde dissolved in binding buffer. In this case, membrane integrity was checked with EH-1 before beginning the staining protocol. Only cultures with <5% EH-1 permeable cells were used.

Statistics

Toxicity experiments were run as triplicates and repeated in at least eight cell preparations. Statistical significances were calculated on the original data sets using the Student's *t*-test. When variances within the compared groups were not homogeneous, the Welch test was applied. Western blots and measurements of $[Ca^{2+}]_i$ were repeated in at least five independent cell preparations.

RESULTS

Role of PARP Activation in NO-Mediated CGC Apoptosis

Activation of PARP, possibly as a consequence of DNA damage, has been suggested to mediate NO toxicity in cortical neurons (16). Here we examined whether PARP activation was involved in Ca^{2+}-mediated CGC apoptosis triggered by NO. Exposure of neurons to different nitric oxide donors or to the potentially terminal cytotoxic mediator peroxynitrite ($ONOO^-$) induced apoptotic cell death. Apoptosis was entirely prevented when MK801 was used to block the NMDA-R, as shown previously (17,18). Kinetics and incidence of apoptosis in neurons derived from PARP −/− mice were not significantly different from those observed in CGC from wild-type mice (Fig. 1). Ca^{2+} influx, fodrin cleavage, and phosphatidylserine translocation occurred in (−/−) neurons as much as in wild-type cells (data not shown). Agents (SNOC or $ONOO^-$) that dissociate rapidly (within seconds) and NO donors that release NO over a period of several hours (DEA-NONOate, spermine-NONOate, GSNO, or SNAP) caused cell death by a mechanism that was entirely dependent on NMDA-R activation and did not involve PARP.

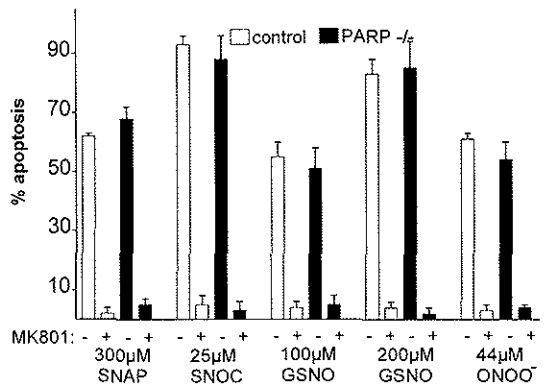

FIG. 1. NO-induced apoptosis in CGC cultures from wild-type and PARP −/− animals

CGC cultures from wild-type (control) or PARP-deficient (PARP −/−) mice were challenged with NO donors as indicated. The percentage of apoptotic neurons was determined after 8 hr by staining with fluorescent chromatin dyes and counting of the cells. Data are means ± SD of triplicate determinations.

Prevention of Cell Death by Caspase Inhibitors

We then examined whether caspase activation was involved in NO-triggered excitotoxic cell death. Inhibitors of caspases effectively prevented neuronal demise induced by slow-release NO donors such as GSNO or SNAP (Fig. 2). When CGC were pretreated with 100 μM of the caspase inhibitors, nuclear condensation, which was completed within 4 hr in neurons treated only with the donors, was prevented. Notably, if at this time the cell culture medium was replaced by normal-conditioned medium, CGC pretreated with caspase inhibitors survived for over 36 hr without evident signs of toxicity. Treatment of cells with z-D-cbk protected ≥85% of the neurons even if the inhibitor was added up to 15 min after GSNO. A structurally related inhibitor, z-F-cmk, which does not inhibit caspases, was not protective (data not shown).

Caspase inhibitors effectively protected from NO-induced excitotoxicity when CGC were challenged with GSNO or SNAP concentrations up to 400 μM. When higher concentrations were used (up to 1000 μM), cell death was still NMDA-R- and Ca^{2+}-dependent (MK801 protected fully), but other degradative pathways, which probably bypassed caspases, were activated (Fig. 3). In line with the hypothesis that the intensity of the insult decided the recruitment of different deg-

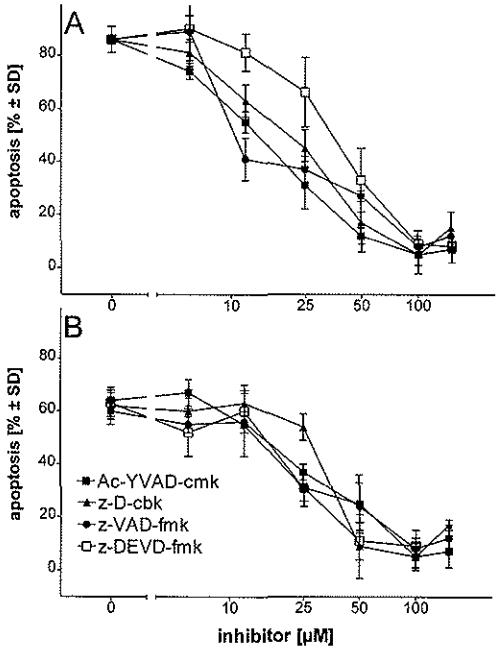

FIG. 2. Protection of CGC from NO toxicity by caspase inhibitors

CGC were incubated with various caspase inhibitors at the concentrations indicated. Thirty minutes later they were challenged with 200 μM GSNO (A) or 350 μM SNAP (B). The percentage of apoptotic neurons was determined by counting the number of cell bodies with condensed chromatin after 8 hr. Data are means ± SD of triplicate determinations.

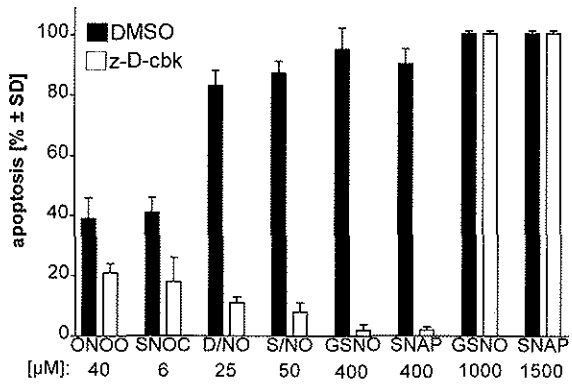

FIG. 3. The role of caspases in different paradigms of NO-triggered cell death

CGC were exposed to increasing concentrations of NO donors with different release kinetics or to $ONOO^-$ for 4 hr. Protection by z-D-cbk was examined. The concentrations of *S*-nitrosocysteine (SNOC), a fast release donor ($t_{1/2} < 10$ min), or $ONOO^-$ were those at which maximum protection was observed. For the donors with intermediate release kinetics ($t_{1/2} = 10–120$ min), DEA-NONOate (D/NO) and spermine-NONOate (S/NO), the highest concentrations are shown, at which >80% protection was observed. For the slow-release ($t_{1/2} > 2$ hr) donors GSNO and SNAP, the highest concentrations are shown, at which complete protection was observed. For the latter group of donors the concentrations at which no protection was observed are also indicated. Notably, toxicity by all donors, at all concentrations shown, was completely prevented by 2 μM MK801. Apoptosis was determined by counting triplicate samples after staining of chromatin with H-33342 and all data were confirmed by MTT measurements, 12 hr after addition of the stimulus.

radative pathways (24) was the observation that apoptosis elicited by fast-releasing NO donors such as SNOC or $ONOO^-$ was only partially prevented by caspase inhibitors (Fig. 3). SNOC and $ONOO^-$ caused a massive and very rapid elevation in $[Ca^{2+}]_i$ [Fig. 4A; (17)]. We then speculated that caspase inhibitors would eventually prevent apoptosis elicited by low, but not by high, concentrations of NO donors, which have a half-life in between those of SNOC and GSNO. Apoptosis induced by NONOates at concentrations <30 μM was indeed completely prevented by z-D-cbk, whereas the caspase inhibitor was ineffective when NONOate concentrations were >150–200 μM. To investigate further the role of caspases in NO-mediated excitotoxicity we then used GSNO, which continuously releases NO over 4 hr (about 120 nM/min at 200 μM) and most closely resembles endogenous NO donors (53).

Caspase Inhibitors Act Downstream to the Ca^{2+} Influx via NMDA-R

To test whether the protection by caspase inhibitors was related to a reduced Ca^{2+} influx through the NMDA-R, we measured $[Ca^{2+}]_i$ in CGC stimulated with different glutamatergic agonists (glutamate, NMDA, kainate) or after chemical depolarization with 50 mM K^+. Caspase inhibitors neither modified the resting $[Ca^{2+}]_i$ nor caused depolarization/agonist-stimulated increases in $[Ca^{2+}]_i$ (data not shown). Moreover, the initial $[Ca^{2+}]_i$ increase triggered by the NO donors was not affected (Fig. 4A). In CGC lethally challenged with NO donors, $[Ca^{2+}]_i$ elevation is sustained over a long period of time (18). This accompanies the appearance of apoptotic nuclei and other features of apoptosis in CGC. To test whether the late Ca^{2+} elevation observed in CGCs undergoing apoptosis was de-

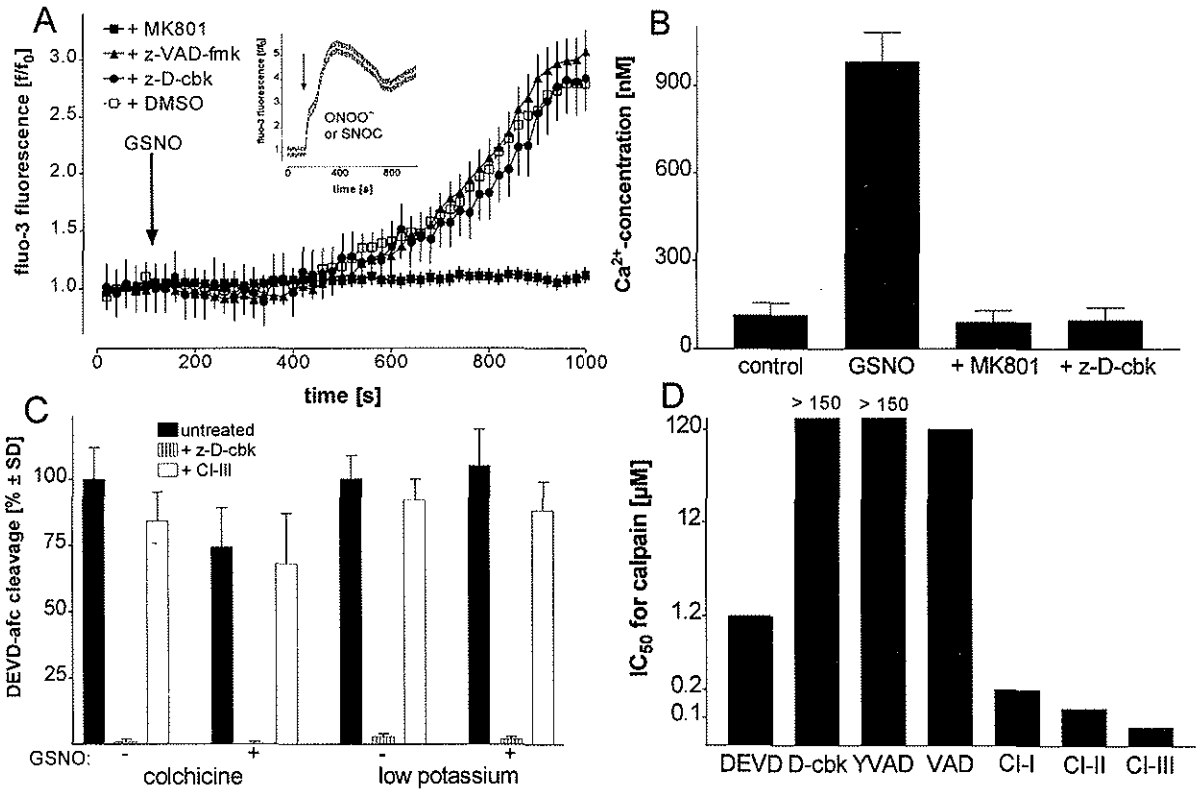

FIG. 4. Caspase inhibitors prevent lethal execution steps downstream of NO-triggered and NMDA-R-mediated $[Ca^{2+}]_i$ increase

(A) CGC were loaded with fluo-3-AM and pretreated with solvent control (DMSO) or 2 μM MK801, 100 μM z-VAD-fmk, or 100 μM z-D-cbk, before they were challenged with GSNO. The increase of $[Ca^{2+}]_i$ in time (f/f_0 fluorescence ratio) was followed by digital videoimaging. For comparison the insert shows the rapid $[Ca^{2+}]_i$ increase following stimulation with SNOC or $ONOO^-$. Data are means ± SEM from 15 to 20 individually recorded neurons. (B) CGC [pretreated with z-D-cbk, MK801, or solvent control (DMSO)] were loaded with fura-2 4 hr after the challenge with 150 μM GSNO. $[Ca^{2+}]_i$ were measured by ratiometric videoimaging and in situ calibration in 60–80 neurons from different preparations. (C) CGC were incubated with 1 μM colchicine in original culture medium or with low potassium medium (5 mM KCl) for 12 hr. Then they were incubated with 200 μM GSNO or PBS in the presence of MK801 for an additional 60 min, before caspase activity was determined. Samples were measured in the absence or presence of z-D-cbk or calpain-inhibitor III (CI-III) as indicated. Data for colchicine or low potassium treatments are presented as relative caspase activities compared with the following controls: colchicine without NO: 1430 U/mg = 100%; low potassium without NO: 2400 U/mg = 100%. (D) Serial dilutions of caspase inhibitors (DEVD = z-DEVD-fmk; D-cbk = z-D-cbk; YVAD = Ac-YVAD-cmk; VAD = z-VAD-fmk) or calpain-inhibitors (CI-I; CI-II, CI-III) were preincubated for 10 min with purified calpain. Calpain activity was measured by a kinetic assay based on the cleavage of suc-LLVY-amc. IC_{50} values were obtained by 4-parameter fit of the inhibition curves.

pendent on caspase activation, $[Ca^{2+}]_i$ was measured 4 hr after exposure to NO donors. In neurons treated with caspase inhibitors and challenged with the NO donors, $[Ca^{2+}]_i$ had returned to the control level (Fig. 4B).

Intracellular Protein Degradation and Chromatin Fragmentation are Prevented by Caspase Inhibitors

To determine intracellular proteolytic activity in neurons challenged with NO donors, we used two distinct approaches. First, we measured caspase activity in lysates of treated cells by following hydrolysis of a fluorogenic peptide substrate (DEVD-afc). Proteolytic activity was induced within 15 to 30 min from the exposure to NO, reached a peak (approximately 200 U/mg) between 45 and 90 min, and declined thereafter (Fig. 5A). This hydrolysis activity was inhibited by pretreatment of CGC with MK801 and it was blocked by z-D-cbk. Since it has recently been suggested that NO may directly inactivate caspases (54), we used two well-characterized

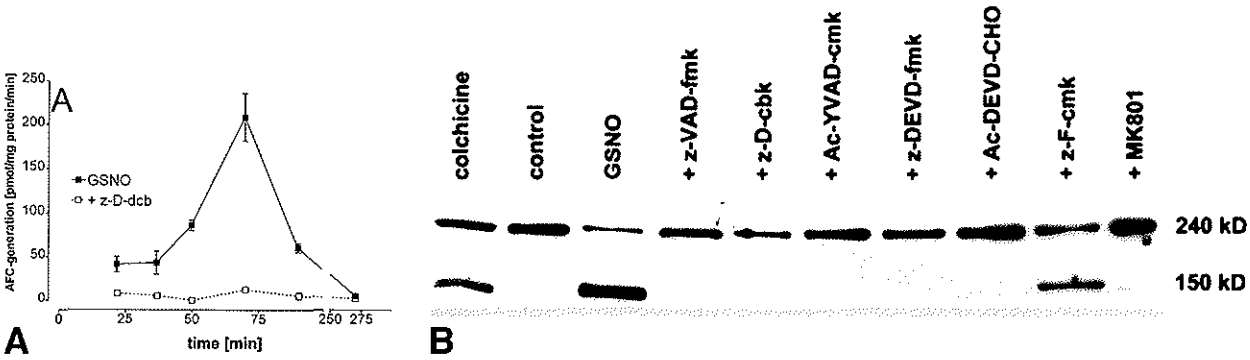

FIG. 5. Prevention of NO-induced intracellular proteolysis by caspase inhibitors

(A) CGC were incubated with 150 μM GSNO and DEVD-afc cleavage activity was determined in cell lysates (in the absence or presence of 1 μM z-D-cbk) after the time points indicated. Data are means ± SD of triplicate determinations. (B) CGC were preincubated for 30 min with 2 μM MK801, 100 μM z-D-cbk, z-VAD-fmk, z-DEVD-fmk, Ac-YVAD-cmk, 1 mM DEVD-CHO, 100 μM z-F-cmk, or solvent control only. Then they were challenged with 200 μM GSNO. Colchicine (1 μM; 12 hr) was used as positive control for induction of CGC apoptosis. After 4 hr, cells were lysed and fodrin proteolysis was determined by immunoblot. Less than 5% of CGC had lost membrane permeability at that time point.

models of CGC apoptosis—that resulting from K^+ withdrawal (34,35) or the apoptosis caused by the microtubule poison colchicine (51,55). In these systems, caspase activity was measured either in the presence or absence of GSNO. As shown in Figure 4C, GSNO did not inhibit or prevent caspase activity in CGC at the concentrations used in this study. Notably, in other culture systems, with higher NO concentrations or under conditions when different NO-related species are possibly formed, NO may directly or indirectly inhibit caspases (54).

In a second approach, we studied a well-characterized proteolytic event occurring in neuronal and non-neuronal apoptosis: the breakdown of fodrin (nonerythroid α-spectrin) (49,56,57). Exposure of CGC to GSNO resulted in fodrin proteolysis, with the formation of a 150-kDa fragment characteristic for caspase-mediated cleavage [i.e., caspase-1 (ICE) or caspase-2 (Nedd-2/ICH-1)]; (57). Fodrin-proteolysis did not occur when NO-treated CGC were preincubated with different caspase inhibitors. In addition, NO-induced fodrin breakdown was also prevented by MK801, which shows that intracellular proteolysis was not directly induced by NO but was rather a downstream consequence of the NMDA-R-mediated Ca^{2+} overload (Fig. 5B).

We also tested whether z-D-cbk would prevent the apoptosis-specific degradation of DNA into high-molecular-weight (HMW) DNA fragments. The caspase inhibitor blocked the formation of 600–50 kbp fragments in a way similar to that of the effect of the NMDA-R antagonist MK801 (Fig. 6). This suggests the involvement of a proteolytic step, downstream to the initial $[Ca^{2+}]_i$ increase, which results in chromatin breakdown.

Caspase Inhibitors did not Affect IL-1β Processing or the Activity of Calpains

In some systems, caspase inhibitors protect cells by preventing the processing and subsequent receptor-mediated actions of IL-1β (39,58). Here, incubation of CGC with 100 ng/ml recombinant murine IL-1β did not result in toxicity and concomitant treatment with GSNO and 10 μg/ml recombinant IL-1 receptor antagonist did not significantly modify neuronal cell death (data not shown).

Preliminary experiments showed that some calpain inhibitors could also protect CGC from GSNO. Since the hydrophobic amino acid at the P2 site of most caspase inhibitors is also a recognition site for calpains, we examined whether the caspase inhibitors used in this study would also inhibit calpain. As shown in Figure 4D, some of the peptides designed as caspase inhibitors were in fact weak calpain inhibitors. However, z-D-cbk or Ac-YVAD-cmk, which strongly protected CGCs from NO-induced apoptosis, were devoid of any calpain inhibitory activity.

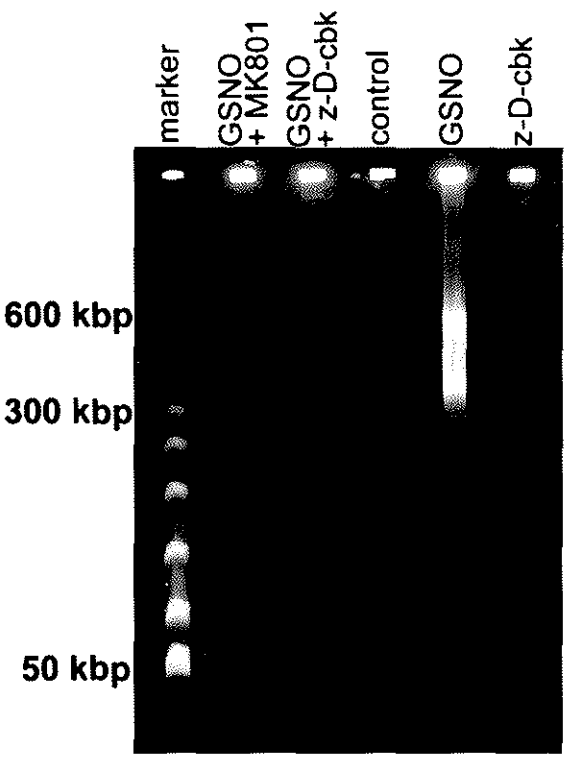

FIG. 6. Prevention of NO-induced chromatin degradation by caspase inhibition

CGC were preincubated for 30 min with 2 μM MK801, 100 μM z-D-cbk, or solvent control only. Then they were challenged with 150 μM GSNO (GSNO + MK801, GSNO + z-D-cbk, GSNO) or they were left unchallenged (z-D-cbk, control). After 4 hr incubations were stopped and DNA fragmentation was analyzed by field-inversion gel electrophoresis. Less than 5% of CGC had lost membrane permeability at that time point.

Apoptosis-Associated Translocation of Phosphatidylserines is Blocked by Caspase Inhibition

Translocation of phosphatidylserine (PS) from the inner to the outer surface of the plasma membrane is an early (52) and specific (51) event in apoptosis, which is not necessarily related to nuclear changes, but it is also dependent on caspase activation (59). In CGC, NO caused PS translocation, as detected by annexin V–staining, within 1 to 2 hr. GSNO-treated neurons stained intensively when the first signs of chromatin condensation were visible and well before the nucleus became pyknotic. CGC remained stainable for several hours until membrane permeability was lost and membranes were degraded. PS translocation was not only seen in cell somata but also in the axonal projections. At GSNO concentrations of ≥150 μM more than 95% of all CGC were annexin-positive and we never observed a neuron with condensed chromatin that had not lost lipid membrane asymmetry. Often, large spherical membrane blebs were formed from the axons, that also stained positively with annexin V and had an intact membrane, as judged from their ability to retain calcein inside. Notably, annexin V–binding to neuronal bodies was completely prevented by MK801, which suggests that PS translocation is also linked to NMDA-R-mediated Ca^{2+} influx and not to direct NO actions. Annexin V–labeling was also inhibited by the caspase inhibitor z-D-cbk, which suggests that caspases are also pivotal for this feature of neuronal apoptosis (Fig. 7).

DISCUSSION

In this study, we used a model of excitotoxicity in which the stimulus is delivered at synaptic sites by an endogenous excitotoxin (17). This does not lead to a rapid breakdown of cellular homeostasis, which would ensue in necrosis (25), and it allows the ordered execution of apoptosis. In this system, we studied the role of PARP and caspases in excitotoxic death of cultured neurons. Our data show that PARP does not play a role in CGC apoptosis induced by six different NO donors. This confirms our previous findings using pharmacological inhibitors of NO (17). However, it differs from findings in some studies using rat cortical neuronal cultures (16). This apparent discrepancy can readily be explained by the fact that NO is not directly lethal for CGC cells but acts via the NMDA receptor, with subsequent $[Ca^{2+}]_i$ increase and apoptosis. The reverse series of events (Ca^{2+}-triggered overproduction of NO) seems to dominate in some (3,5), but not in other, (60–62) models of neurotoxicity, and may reflect the involvement of different execution mechanisms.

Here, the initiating step in NO-induced CGC apoptosis is the induction of $[Ca^{2+}]_i$ overload (17,18). Further support for this model comes from the observation that not only cell death and nuclear alterations but also intracellular proteolysis, HMW-DNA fragmentation, and translocation of PS to the outer surface of the plasma membrane occurred downstream of the Ca^{2+} influx. It is apparent that none of these processes was directly triggered by NO.

A caspase-like proteolytic activity seems to be the main death executor, which ties NO-in-

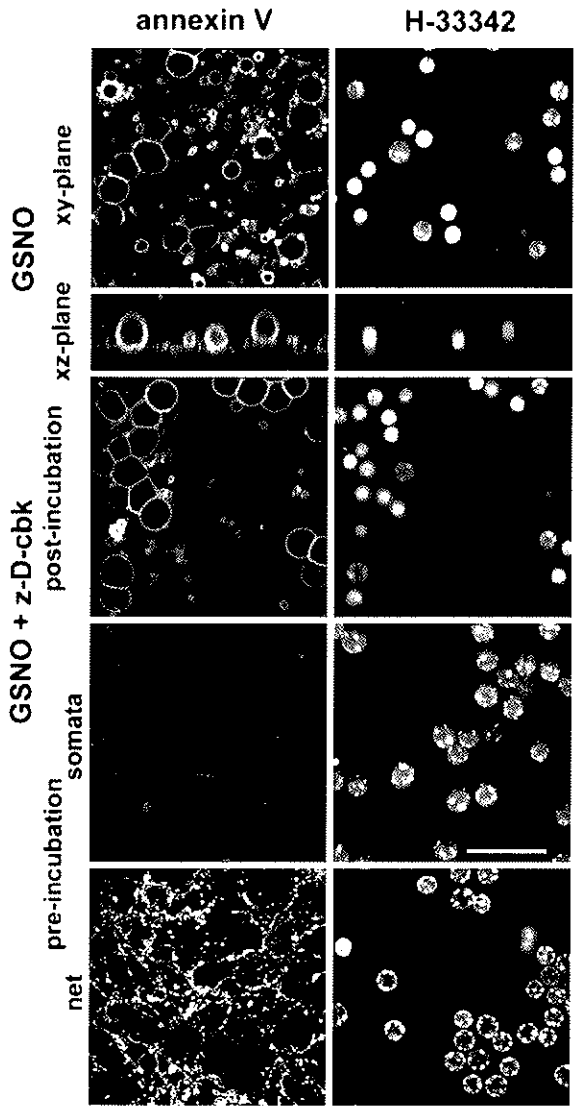

FIG. 7. Prevention of NO-induced apoptotic phosphatidylserine translocation by caspase inhibition

CGC were incubated with GSNO for 2 hr before they were stained with FITC–annexin V and H-33342 and imaged by confocal microscopy. The top panel shows an xy-section through the cell bodies (4 μm from coverslip). Apoptotic nuclei appear condensed and hyperfluorescent and are surrounded by annexin V–stained membranes. A transversal section (xz-plane) demonstrates that the entire surface of the apoptotic neurons *plus* some nonchromatin-containing blebs formed from the axonal projections are surface-stained with annexin V. Neurons that had been preincubated with z-D-cbk did not condense and did not stain with annexin V (preincubation somata). The axonal net (0.7 μm from coverslip) of neurons protected by z-D-cbk stained focally with annexin V, possibly suggesting synaptic activity (preincubation-net). CGC that were challenged with GSNO and received z-D-cbk only during the last 30 min of the incubation were not protected and stained positively with annexin V (postincubation).

duced $[Ca^{2+}]_i$ overload with the appearance of apoptosis. This assumption is based on the findings that caspase inhibitors prevented neither Ca^{2+} influx through glutamate receptors nor NO-dependent NMDA receptor activation. However, they blocked proteolysis, chromatin degradation, PS exposure, and cell death. Moreover, blockage of the NMDA-R prevented caspase-like proteolytic activity and all the resulting downstream events. This places caspase activation between NMDA-R-mediated Ca^{2+} influx and the appearance of the typical apoptotic features. The finding that neurons protected by the caspase inhibitors survived for days suggests that caspase activation is situated at, or upstream of, the commitment step in neuronal death, at least in this experimental system.

Preliminary data in the same experimental system suggest that calpains can also be involved in NO-induced CGC apoptosis. Therefore, to avoid artifactual effects, we used four structurally different caspase inhibitors and tested their ability to inhibit calpains. Our results showed that the most effective caspase inhibitors did not affect calpain activity. Accordingly, these inhibitors prevented caspase-specific proteolytic events such as DEVD-afc hydrolysis and fodrin cleavage. A common indicator of caspase activity, PARP-cleavage, seems to be neither relevant (51) nor always correlated with apoptosis (56,63, and this study). On the other hand, fodrin, a cytoskeletal-associated protein, is one of the caspase substrates that is most relevant to apoptosis and neuropathology, although it is difficult to establish whether fodrin is directly cleaved by caspases or by other downstream proteolytic systems (64). The typical pattern of fodrin cleavage by caspase 3 includes a degradation product with a size of 120 kDa. We detected this fragment in CGC undergoing apoptosis after treatment with colchicine or K^+ deprivation, but not after exposure to NO-donors. Fodrin cleavage in NO-treated neurons was more likely operated by caspase-1 or caspase-2, which only yield the 150 kDa fragment (57). The lack of relevant caspase 3-activation in CGC exposed to GSNO is corroborated also by the finding of a relatively low DEVD cleavage activity. Predominant activation of caspase-2, which has been previously implicated in neuronal apoptosis (35,63,65), would explain the low DEVD-afc cleavage activity and perhaps the different nuclear morphology of GSNO-treated CGC when compared with that observed in apoptosis induced by low K^+, where

caspase-3 seems to be the predominant proteolytic enzyme (33).

While high-molecular-weight DNA fragmentation has been found in virtually all forms of apoptotic cell death, DNA laddering is a dispensable consequence of chromatin degradation (66). Prevention by z-D-cbk of GSNO-induced formation of 600-, 300-, and 50-kbp DNA fragments suggests the involvement of caspases in this process, downstream of raised $[Ca^{2+}]_i$. A similar conclusion can be derived when examining PS translocation. This process seems to be an early event (52) specific for the apoptotic, but not for the necrotic, demise (67). In non-neuronal cells, PS translocation seems to be independent of increases in $[Ca^{2+}]_i$ (68), but it requires caspase activation (59). Here, we extended this concept to neurons and showed that caspase activation is linked to the alterations in membrane lipid asymmetry also in apoptosis of CGC.

Developmental neuronal death or neuronal demise due to growth factor withdrawal have been considered as conceptually and biochemically different types of death from that observed in excitotoxicity. The role of caspases in the execution of apoptosis elicited by growth factor withdrawal or in paradigms of developmental cell death has been firmly established, whereas such clear evidence has been amiss in models of excitotoxic neuronal injury. In fact, neuronal apoptosis has often been opposed to the demise induced by glutamate, which was supposed to lack the regulated series of events involved in a death program (23,69–71). This view is now challenged by an increasingly large body of evidence: apoptotic cell death is indeed a feature of many stroke models (27–30,72) in which caspase inhibitors reduced the extent of damage (36,37). Oxidative stress, hypoxia, exposure to nitropropionic acid, 4-hydroxynonenal, or MPP^+, epileptic seizures, trauma, or exposure to HIV gp120, which are closely associated with the onset of excitotoxicity, have been repeatedly shown to cause neural apoptosis (38,71,73–76). Finally, apoptosis has been observed directly in neurons exposed to excess glutamate or in models, including the one described here, of endogenous excitotoxicity (17,18,24,25,77). The discrepancy of findings and views may be reconciled by the consideration that excitotoxic mediators can induce either apoptosis or necrosis, depending on the intensity of stimulation (24,25). A further source of contrasting interpretations has originated from the significance attributed to different morphological appearances of apoptotic neurons. Glutamate-induced apoptotic nuclear changes are characterized by typical chromatin condensation and nuclear pyknosis with the biochemical correlate of HMW-DNA fragmentation, whereas oligonucleosomal DNA fragmentation and nuclear fragmentation are less apparent (25). In contrast, neurons exposed to low K^+, staurosporine, or 4-hydroxynonenal exhibit the typical DNA laddering and nuclear fragmentation. For this reason, excitotoxic neuronal death has often been described as nonapoptotic (69–71), although it is now well established that oligonucleosomal DNA fragmentation and nuclear fragmentation are late and dispensable events in apoptosis (66).

The shape of cell death is controlled by multiple factors (26). Several forms and subroutines of the death program might have evolved because of their significance for tissues and organs and may not be common to all apoptosis models. For example, Ca^{2+} overload, a common feature in excitotoxicity, but not in models of growth factor deprivation, may trigger downstream events that preclude the completion of nuclear fragmentation. In extreme cases, rapid breakdown of $[Ca^{2+}]_i$ homeostasis may even prevent the execution of any of the organized events leading to apoptosis and therefore result in necrosis (25). When the Ca^{2+} overload is slow and relatively moderate (as in CGC exposed to low GSNO concentrations), caspase activation has a predominant role in the execution of the cell death program. Notably, under these circumstances, caspase inhibitors abolish the late $[Ca^{2+}]_i$ elevation observed in dying neurons, although the initial Ca^{2+} influx through NMDA-Rs is unaffected (see Fig. 4B). On the other hand, when CGC are exposed to high GSNO concentrations, to NO donors that cause a rapid Ca^{2+} influx (such as SNOC), or to excess glutamate, we still observe clear nuclear condensation, HMW-DNA fragmentation, prevention of cell death by NMDA-R antagonists (18,17,25), and outer membrane translocation of PS. However, in this case, caspase inhibitors are hardly protective, although the overall mode of cell death does not change. With even stronger insults, the degradative processes typical of apoptosis do not occur and neurons die by necrosis (24,25). Evidence that cells triggered to undergo apoptosis are instead forced to die by necrosis when energy levels are rapidly compromised has been recently provided (25,51). These findings may explain the observation that multiple shapes of neuronal death can appear concomitantly in vivo. More-

over, our results support the notion (36,37) that caspase inhibition may be a useful approach for intervention in processes involving excitotoxicity and provide further information on the relevant targets of these substances in neurons.

ACKNOWLEDGMENTS

We are grateful to Dr. Zhao Qi Wang for the gift of the PARP (−/−) mice and for helpful discussion and comments on the manuscript. The excellent technical assistance of H. Naumann, T. Schmitz, and B. Kartmann is gratefully acknowledged. We thank Dr. T. Hartung for providing IL-1β and IL-1RA and H. Hentze for help with caspase measurements. This study was supported by the University of Konstanz AFF grant 27/95, the DFG grant Ni519/1-1, and the EEC grants ENV4-CT96-0169 and 12029-97-06 F1ED ISP D.

REFERENCES

1. Beckman JS, Koppenol WH. (1996) Nitric oxide, superoxide, and peroxynitrite: The good, the bad, and the ugly. *Am. J. Physiol.* **271:** C1424–C1437.
2. Garthwaite J, Boulton CL. (1995) Nitric oxide signaling in the central nervous system. *Annu. Rev. Physiol.* **57:** 683–706.
3. Zhang J, Snyder SH. (1995) Nitric oxide in the nervous system. *Annu. Rev. Pharmacol. Toxicol.* **35:** 213–233.
4. Huang PL, Fishman MC. (1996) Genetic analysis of nitric oxide synthase isoforms: Targeted mutation in mice. *J. Mol. Med.* **74:** 415–421.
5. Sandani AF, Dawson TM, Dawson VL. (1997) Nitric oxide synthase in models of focal ischemia. *Stroke* **28:** 1283–1288.
6. Snyder SH. (1996) No NO prevents parkinsonism. *Nature Med.* **2:** 965–966.
7. Schulz JB, Matthews RT, Jenkins BG, Ferrante RJ, Siwek D, Henshaw DR, Cipolloni PB, Mecocci P, Kowall NW, Rosen BR, Beal MF. (1995) Blockade of neuronal nitric oxide synthase protects against excitotoxicity in vivo. *J. Neurosci.* **15:** 8419–8429.
8. Galpern WR, Matthews RT, Beal FM, Isacson O. (1996) NGF attenuates 3-nitrotyrosine formation in a 3-NP model of Huntington's disease. *NeuroReport* **7:** 2639–2642.
9. Schulz JB, Huang PL, Matthews RT, Passov D, Fishman MC, Beal MF. (1996) Striatal malonate lesions are attenuated in neuronal nitric oxide synthase knockout mice. *J. Neurochem.* **67:** 430–433.
10. Lipton SA, Choi Y-B, Pan Z-H, Lei SZ, Chen H-SV, Sucher NJ, Loscalzo J, Singel DJ, Stamler JS. (1993) A redox-based mechanism for the neuroprotective and neurodestructive effects of nitric oxide and related nitroso-compounds. *Nature* **364:** 626–632.
11. Stamler JS. (1994) Redox signaling: Nitrosylation and related target interactions of nitric oxide. *Cell* **78:** 931–936.
12. Stamler JS, Jia L, Eu JP, McMahon TJ, Demchenko IT, Bonaventura J, Gernert K, Piantadosi CA. (1997) Blood flow regulation by S-nitrosohemoglobin in the physiological oxygen gradient. *Science* **276:** 2034–2037.
13. Meffert MK, Calakos NC, Scheller RH, Schulman H. (1996) Nitric oxide modulates synaptic vesicle docking/fusion reactions. *Neuron* **16:** 1229–1236.
14. Meffert MK, Premack BA, Schulman H. (1994) Nitric oxide stimulates calcium-independent synaptic vesicle release. *Neuron* **12:** 1235–1244.
15. Gross SS, Wolin MS. (1995) Nitric oxide: Pathophysiological mechanisms. *Annu. Rev. Physiol.* **57:** 737–769.
16. Zhang J, Dawson VL, Dawson TM, Snyder SH. (1994) Nitric oxide activation of poly-(ADP-ribose) synthetase in neurotoxicity. *Science* **263:** 687–689.
17. Leist M, Fava E, Montecucco C, Nicotera P. (1997) Peroxynitrite and NO-donors induce neuronal apoptosis by eliciting autocrine excitotoxicity. *Eur. J. Neurosci.* **9:** 1488–1498.
18. Bonfoco E, Leist M, Zhivotovsky B, Orrenius S, Lipton SA, Nicotera P. (1996) Cytoskeletal breakdown and apoptosis elicited by NO-donors in cerebellar granule cells require NMDA-receptor activation. *J. Neurochem.* **67:** 2484–2493.
19. Choi DW. (1988) Glutamate neurotoxicity and diseases of the nervous system. *Neuron* **1:** 623–634.
20. Choi DW. (1995) Calcium: Still center-stage in hypoxic-ischemic neuronal death. *Trends Neurosci.* **18:** 58–60.
21. Meldrum B, Garthwaite J. (1990) Excitatory amino acid neurotoxicity and neurodegenerative disease. *Trends Pharmacol. Sci.* **11:** 379–387.
22. Leist M, Nicotera P. (1997) Calcium and neural death. *Rev. Physiol. Pharmacol. Biochem.* **132:** 79–125.

23. Koh J-Y, Gwag BJ, Lobner D, Choi DW. (1995) Potentiated necrosis of cultured cortical neurons by neurotrophins. *Science* **268:** 573–575.
24. Bonfoco E, Krainc D, Ankarcrona M, Nicotera P, Lipton SA. (1995) Apoptosis and necrosis: Two distinct events induced respectively by mild and intense insults with NMDA or nitric oxide/superoxide in cortical cell cultures. *Proc. Natl. Acad. Sci. U.S.A.* **92:** 72162–72166.
25. Ankarcrona M, Dypbukt JM, Bonfoco E, Zhivotovsky B, Orrenius S, Lipton SA, Nicotera P. (1995) Glutamate-induced neuronal death: A succession of necrosis or apoptosis depending on mitochondrial function. *Neuron* **15:** 961–973.
26. Nicotera P, Leist M. (1997) Energy supply and the shape of death in neurons and lymphoid cells. *Cell Death Differ.* **4:** 435–442.
27. Portera-Cailliau C, Hedreen JC, Price DL, Koliatsos VE. (1995) Evidence for apoptotic cell death in Huntington disease and excitotoxic animal models. *J. Neurosci.* **15:** 3775–3787.
28. Li Y, Chopp M, Jiang N, Yao F, Zaloga C. (1995) Temporal profile of in situ DNA fragmentation after transient middle cerebral artery occlusion in the rat. *J. Cereb. Blood Flow Metab.* **15:** 389–397.
29. Charriaut-Marlangue C, Margaill I, Borrega F, Plotkine M, Ben-Ari Y. (1996) NG-Nitro-L-arginine methyl ester reduces necrotic but not apoptotic cell death induced by reversible focal ischemia in rat. *Eur. J. Pharmacol.* **310:** 137–140.
30. Beilharz EJ, Williams CE, Dragunow M, Sirimanne ES, Gluckman PD. (1995) Mechanisms of delayed cell death following hypoxic-ischemic injury in the immature rat: Evidence for apoptosis during selective neuronal loss. *Mol. Brain Res.* **29:** 1–14.
31. Henkart PA. (1996) ICE family proteases: mediators of all apoptotic cell death? *Immunity* **4:** 195–201.
32. Zhivotovsky B, Burgess DH, Vanags DM, Orrenius S. (1997) Involvement of cellular proteolytic machinery in apoptosis. *Biochem. Biophys. Res. Commun.* **230:** 481–488.
33. Armstrong RC, Aja TJ, Hoang KD, Gaur S, Bai X, Alnemri ES, Litwack G, Karanewsky DS, Fritz LC, Tomaselli KJ. (1997) Activation of the Ced3/ICE-related protease CPP32 in cerebellar granule neurons undergoing apoptosis but not necrosis. *J. Neurosci.* **17:** 553–562.
34. Schulz JB, Weller M, Klockgether T. (1996) Potassium deprivation-induced apoptosis of cerebellar granule neurons: a sequential requirement for new mRNA and protein synthesis, ICE-like protease activity, and reactive oxygen species. *J. Neurosci.* **16:** 4696–4706.
35. Lynch T, Vasilakos JP, Raser K, Keane KM, Shivers BD. (1997) Inhibition of the interleukin-1 beta converting enzyme family rescues neurons from apoptotic death. *Mol. Psychiatry* **2:** 227–238.
36. Hara H, Friedlander RM, Gagliardini V, Ayata C, Fink K, Huang Z, Shimizu-Sasamata M, Yuan J, Moskowitz MA. (1997) Inhibition of interleukin 1beta converting enzyme family proteases reduces ischemic and excitotoxic neuronal damage. *Proc. Natl. Acad. Sci. U.S.A.* **94:** 2007–2012.
37. Loddick SA, MacKenzie A, Rothwell NJ. (1996) An ICE inhibitor, z-VAD-DCB attenuates ischaemic brain damage in the rat. *NeuroReport* **7:** 1465–1468.
38. Yakovlev AG, Knoblach SM, Fan L, Fox GB, Goodnight R, Faden AI. (1997) Activation of CPP32-like caspases contributes to neuronal apoptosis and neurological dysfunction after traumatic brain injury. *J. Neurosci.* **17:** 7415–7424.
39. Friedlander RM, Gagliardini V, Rotello RJ, Yuan J. (1996) Functional role of interleukin-1β (IL-1β) in IL-1β converting enzyme-mediated apoptosis. *J. Exp. Med.* **184:** 717–724.
40. Beckman JS, Chen J, Ischiropoulos H, Crow JP. (1995) Oxidative chemistry of peroxynitrite. *Methods Enzymol.* **233:** 229–240.
41. Hart TW. (1985) Some observations concerning the S-nitroso and S-phenysulfonyl derivatives of L-cysteine and glutathione. *Tetrahedron Lett.* **26:** 2013–2016.
42. Field L, Dilts RV, Ravichandran R, Lenhert PG, Carnahan GE. (1978) An unusually stable thionitrite from *N*-acetyl-D,L-penicillamine; X-ray crystal and molecular structure of 2-(Acetylamino)-2-carboxy-1,1-dimethylethyl thionitrite. *J. C. S. Chem. Commun.* 249–250.
43. Lei SZ, Pan Z-H, Aggarwal SK, Chen H-SV, Hartman J, Sucher NJ, Lipton SA. (1992) Effect of nitric oxide production on the redox modulatory site of the NMDA receptor-channel complex. *Neuron* **8:** 1087–1099.

44. Wang Z-Q, Auer B, Stingl L, Berghammer H, Haidacher D, Schweiger M, Wagner EF. (1995) Mice lacking ADPRT and poly(ADP-ribosyl)ation develop normally but are susceptible to skin disease. *Genes Dev.* **9:** 509–520.
45. Schousboe A, Meier E, Drejer J, Hertz L. (1989) Preparation of primary cultures of mouse (rat) cerebellar granule cells. In: Shahar A, de Vellis J, Vernadakis A, Haber B (eds). *A Dissection and Tissue Culture Manual of the Nervous System.* Alan R. Liss, New York, pp. 203–206.
46. Mosmann T. (1983) Rapid colorimetric assay for cellular growth and survival: Application to proliferation and cytotoxicity assays. *J. Immunol. Methods* **65:** 55–63.
47. Grynkiewicz G, Poenie M, Tsien RY. (1985) A new generation of Ca^{2+} indicators with greatly improved fluorescence properties. *J. Biol. Chem.* **260:** 3440–3450.
48. Thomas AP, Delaville F. (1991) The use of fluorescent indicators for measurements of cytosolic free calcium concentrations in cell populations and single cells. In: McCormack JG, Cobbold PH (eds). *Cellular Calcium.* Oxford University Press, Oxford, pp. 1–54.
49. Martin SJ, O'Brien GA, Nishioka WK, McGahon AJ, Mahboubi A, Saido TC, Green DR. (1995) Proteolysis of Fodrin (non-erythroid spectrin) during apoptosis. *J. Biol. Chem.* **270:** 6425–6428.
50. Thornberry NA. (1994) Interleukin-1 beta converting enzyme. *Methods Enzymol.* **244:** 615–631.
51. Leist M, Single B, Künstle G, Volbracht C, Hentze H, Nicotera P. (1997) Apoptosis in the absence of poly-(ADP-ribose) polymerase. *Biochem. Biophys. Res. Commun.* **233:** 518–522.
52. Koopman G, Reutelingsperger CPM, Kuijten GAM, Keehnen RMJ, Pals ST, van Oers MHJ. (1994) Annexin V for flow cytometric detection of phosphatidylserine expression on B cells undergoing apoptosis. *Blood* **84:** 1415–1420.
53. Do KQ, Benz B, Grima G, Gutteck-Amsler U, Kluge I, Salt TE. (1996) Nitric oxide precursor arginine and S-nitrosoglutathione in synaptic and glial function. *Neurochem. Int.* **29:** 213–224.
54. Dimmeler S, Haendeler J, Nehls M, Zeiher AM. (1997) Suppression of apoptosis by nitric oxide via inhibition of interleukin-1beta-converting enzyme (ICE)-like and cysteine protease protein (CPP)-32-like proteases. *J. Exp. Med.* **185:** 601–607.
55. Bonfoco E, Ceccatelli S, Manzo L, Nicotera P. (1995) Colchicine induces apoptosis in cerebellar granule cells. *Exp. Cell Res.* **218:** 189–200.
56. Cryns VL, Bergeron L, Zhu H, Li H, Yuan J. (1996) Specific cleavage of alpha-fodrin during fas- and tumor necrosis factor-induced apoptosis is mediated by an interleukin-1 beta-converting enzyme/Ced-3 protease distinct from the poly(ADP-ribose) polymerase protease. *J. Biol. Chem.* **271:** 31277–31282.
57. Nath R, Raser KJ, Stafford D, Hajimohammadreza I, Rosner A, Allen H, Talanian RV, Yuen P, Gilbertsen RB, Wang KKW. (1996) Non-erythroid alpha-spectin breakdown by calpain and interleukin 1beta-converting-enzyme-like protease(s) in apoptotic cells: Contributory roles of both protease families in neuronal apoptosis. *Biochem. J.* **319:** 683–690.
58. Troy CM, Stefanis L, Prochiantz A, Greene LA, Shelanski ML. (1996) The contrasting roles of ICE family proteases and interleukin-1beta in apoptosis induced by trophic factor withdrawal and by copper/zinc superoxide dismutase down-regulation. *Proc. Natl. Acad. Sci. U.S.A.* **93:** 5635–5640.
59. Martin SJ, Finucane DM, Amarante-Mendes GP, O'Brien GA, Green DR. (1996) Phosphatidylserine externalization during CD95-induced apoptosis of cells and cytoplasts requires ICE/CED-3 protease activity. *J. Biol. Chem.* **271:** 28753–28756.
60. Hewett SJ, Corbett JA, McDaniel ML, Choi DW. (1993) Inhibition of nitric oxide formation does not protect murine cortical cell cultures from *N*-methyl-D-aspartate neurotoxicity. *Brain Res.* **625:** 337–341.
61. Regan R, Renn K, Panter SS. (1993) NMDA neurotoxicity in murine cortical cell cultures is not attenuated by hemoglobin or inhibition of nitric oxide synthesis. *Neurosci. Lett.* **153:** 53–56.
62. Garthwaite G, Garthwaite J. (1994) Nitric oxide does not mediate acute glutamate neurotoxicity, nor is it neuroprotective, in rat brain slices. *Neuropharmacology* **33:** 1431–1438.
63. Stefanis L, Park DS, Yan CYI, Farinelli SE, Troy CM, Shelanski ML, Greene LA. (1996) Induction of CPP32-like activity in PC12 cells by withdrawal of trophic support. Dis-

sociation from apoptosis. *J. Biol. Chem.* **271:** 30663–30671.
64. Siman R, Noszek JC. (1988) Excitatory amino acids activate calpain I and induce structural protein breakdown in vivo. *Neuron* **1:** 279–287.
65. Troy CM, Stefanis L, Greene LA, Shelanski ML. (1997) Nedd2 is required for apoptosis after trophic factor withdrawal, but not superoxide dismutase (SOD1) downregulation, in sympathetic neurons and PC12 cells. *J. Neurosci.* **17:** 1911–1918.
66. Leist M, Nicotera P. (1997) The shape of cell death. *Biochem. Biophys. Res. Commun.* **236:** 1–9.
67. Leist M, Single B, Castoldi AF, Kühnle S, Nicotera P. (1997) Intracellular ATP concentration: A switch deciding between apoptosis and necrosis. *J. Exp. Med.* **185:** 1481–1486.
68. Hampton MB, Vanags DM, Pörn-Ares I, Orrenius S. (1996) Involvement of extracellular calcium in phosphatidylserine exposure during apoptosis. *FEBS Lett.* **399:** 277–282.
69. MacManus JP, Rasquinha I, Black MA, Laferriere NB, Monette R, Walker T, Morley P. (1997) Glutamate-treated rat cortical neuronal cultures die in a way different from the classical apoptosis induced by staurosporine. *Exp. Cell Res.* **233:** 310–320.
70. Gwag BJ, Lobner D, Koh JY, Wie MB, Choi DW. (1995) Blockade of glutamate receptors unmasks neuronal apoptosis after oxygene-glucose deprivation in vitro. *Neuroscience* **68:** 615–619.
71. Pang Z, Geddes JW. (1997) Mechanisms of cell death induced by the mitochondrial toxin 3-nitropropionic acid: Acute excitotoxic necrosis and delayed apoptosis. *J. Neurosci.* **17:** 3064–3073.
72. Charriaut-Marlangue C, Margaill I, Plotkine M, Ben-Ari Y. (1995) Early endonuclease activation following reversible focal ischemia in the rat brain. *J. Cereb. Blood Flow Metab.* **15:** 385–388.
73. Kruman I, Bruce-Keller AJ, Bredesen D, Waeg G, Mattson MP. (1997) Evidence that 4-hydroxynonenal mediates oxidative stress-induced neuronal apoptosis. *J. Neurosci.* **17:** 5089–5100.
74. Rink A, Fung K-M, Trojanowski JQ, Lee VM-Y, Neugebauer E, McIntosh TK. (1995) Evidence of apoptotic cell death after experimental traumatic brain injury in the rat. *Am. J. Pathol.* **147:** 1575–1583.
75. Dipasquale B, Marini AM, Youle RJ. (1991) Apoptosis and DNA degradation induced by 1-methyl-4-phenylpyridinium in neurons. *Biochem. Biophys. Res. Commun.* **181:** 1442–1448.
76. Charriaut-Marlangue C, Aggoun-Zouaoui D, Represa A, Ben-Ari Y. (1996) Apoptotic features of selective neuronal death in ischemia, epilepsy and gp120 toxicity. *Trends Neurosci.* **19:** 109–114.
77. Kure S, Tominaga T, Yoshimoto T, Tada K, Narisawa K. (1991) Glutamate triggers internucleosomal DNA cleavage in neuronal cells. *Biochem. Biophys. Res. Commun.* **179:** 39–45.